PROCEEDINGS of the
23rd International Congress on Acoustics

9 to 13 September 2019 in Aachen, Germany

Prediction of dynamic hub forces as a source of structure-borne tire/coarse road noise using a high-fidelity simulation approach

Daniel DE GREGORIIS(1,2)*, Frank NAETS(1,3)†, Peter KINDT(2)‡, Wim DESMET(1,3)§

(1)KU Leuven, Belgium

(2)Goodyear Innovation Center* Luxembourg, Luxembourg

(3)DMMS Lab, Flanders Make, Belgium

Abstract

When optimizing the tire/road structure-borne interior noise, multiple other coupled tire performances need to be simultaneously optimized. Typically, different tire design prototypes are built and tested. However, with the recent advent in virtual product development and the Digital Twin concept, high-fidelity numerical simulation approaches become a viable alternative to the experimental approach. These numerical approaches allow for design space exploration without the need for building and testing physical tire prototypes. Therefore, in this work the use of a fully predictive nonlinear numerical approach for the prediction of the dynamic contact- and hub forces of a tire rolling over a coarse road surface is described. These predicted hub forces can then be further used to assess the tire/road structure-borne noise performance of a tire. The influence of incorporating tire model nonlinearities as well as rim flexibility on the simulated hub forces is discussed. Furthermore, nonlinear model order reduction and hyper-reduction techniques are applied to greatly reduce the numerical simulation time, being approximately ten times faster than the experimental approach. Finally, a comparison between the predicted hub forces and experimental hub forces is shown, where a sufficient correspondence between both can be observed for design engineering purposes.

Keywords: Tire, Interior noise, Simulation

1 INTRODUCTION

In this work, the prediction of dynamic hub forces arising due to a tire rolling with a constant speed (i.e. steady-state) over a coarse road surface is of interest. These hub forces are typically a main source of structure-borne interior cabin noise for the 0 – 400Hz range (1, 2). The structure-borne interior noise tends to dominates the airborne interior noise in this frequency range for rolling over a coarse road surface (1, 3, 4). The ability to predict the hub forces and corresponding structure-borne noise of a specific tire design is therefore valuable in an overall performance assessment during virtual tire development. More specifically, the vertical hub force is of interest as a performance indicator of the structure-borne interior noise performance of a tire design. As the tread pattern has limited contribution to the hub forces below 400Hz for rolling over a coarse road surface(1), only slick and ribbed slick tires are considered in this work. Recently, the authors have proposed a fully predictive methodology for simulating dynamic contact and hub forces for rolling over a coarse road surface (5). Here, a fully nonlinear structural finite element (FE) tire model in combination with the Arbitrary Lagrangian Eulerian (ALE) formulation for bodies in rolling contact (6), an acoustic FE model of the air cavity, a constraint-based contact formulation (7) and a hyper-reduction method are used. In this work, the methodology is extended to include the rotation of the air cavity as well. In earlier work (5) the regular Helmholtz equation was applied which corresponds to assuming a non-rotating air cavity. In this work, the acoustic domain

*daniel.degregoriis@kuleuven.be
†frank.naets@kuleuven.be
‡peter_kindt@goodyear.com
§wim.desmet@kuleuven.be

is modeled using the convected Helmholtz equation (8), similar to the work by e.g. Cao and Bolton (9). A nonlinear FE tire model can be seen as a virtual replica (or Digital Twin (10)) of the real tire, thus allowing a design engineer to directly apply the same changes to this model as would be done to a physical tire design. Examples of such design changes are reinforcement fiber angles, compound properties etc. The use of a fully nonlinear FE tire model is typically computationally too expensive to use in a design context, as it often takes more time to run the simulations than to build the physical tire prototypes. Therefore, the a-priori nonlinear Multi-Expansion Modal (MEM) hyper-reduction method (11) is applied to the nonlinear FE tire model, greatly reducing the computational costs and enabling the use of the fully predictive method as an alternative to the experimental testing. The remainder of this work is structured as follows: the high-fidelity tire modeling approach is discussed in section 2. Application of the MEM hyper-reduction method is discussed in section 3. The use of the predictive methodology to estimate the structure-borne interior noise performance of a test tire is discussed in section 4. Finally, conclusions are given in section 5.

2 HIGH-FIDELITY TIRE MODELING FOR HUB FORCE PREDICTION

As discussed in section 1, a high-fidelity tire modeling approach is adopted (5). The semi-discretized FE equations of motion of the structural tire domain can be expressed as:

$$\mathbf{M}\ddot{\mathbf{x}} + \mathbf{G}_{\mathbf{ALE}}(\mathbf{x},\omega)\dot{\mathbf{x}} + \mathbf{f}(\mathbf{x},\dot{\mathbf{x}}) - \mathbf{f}_{\mathbf{ALE}}(\mathbf{x},\omega) = \mathbf{f}_{\mathbf{p}}(\mathbf{x},p_a) + \mathbf{f}_{\mathbf{c}}(\mathbf{x},\mathbf{x}_{\mathbf{r}}) + \mathbf{f}_{\mathbf{e}} \tag{1}$$

Here, the current configuration $\mathbf{x}(t) \in \mathbb{R}^n$ is defined as $\mathbf{x}(t) = \mathbf{x}_0 + \mathbf{u}(t)$, where $\mathbf{x}_0$ is a reference configuration and $\mathbf{u}(t)$ is the total displacement with respect to the reference configuration at time t. The first and second derivatives of the current configuration with respect to time are denoted as $\dot{\mathbf{x}}$ and $\ddot{\mathbf{x}}$, respectively. All configuration-dependent terms therefore depend on time as well, but this time-dependency is dropped from notation for clarity reasons. The constant mass matrix is denoted by $\mathbf{M} \in \mathbb{R}^{n\times n}$, the Gyroscopic ALE matrix is denoted by $\mathbf{G}_{\mathbf{ALE}}(\mathbf{x},\omega) \in \mathbb{R}^{n\times n}$, the nonlinear internal force term is denoted by $\mathbf{f}(\mathbf{x},\dot{\mathbf{x}}) \in \mathbb{R}^n$ (12), the ALE rotational inertial force term is denoted by $\mathbf{f}_{\mathbf{ALE}}(\mathbf{x},\omega) \in \mathbb{R}^n$, where ω is the constant angular velocity of the tire, the nonlinear inflation pressure force term is denoted as $\mathbf{f}_{\mathbf{p}}(\mathbf{x},p_a) \in \mathbb{R}^n$ (12), where p_a denotes the tire inflation pressure, the nonlinear contact force term is denoted as $\mathbf{f}_{\mathbf{c}}(\mathbf{x},\mathbf{x}_{\mathbf{r}}) \in \mathbb{R}^n$, where $\mathbf{x}_{\mathbf{r}}$ is the set of road surface contact constraints at time t, and the constant external force term (e.g. a vertical load) is denoted as $\mathbf{f}_{\mathbf{e}} \in \mathbb{R}^n$. As slick and ribbed slick tires rolling with a constant angular velocity over a coarse road surface are considered in this work, the Arbitrary Lagrangian Eulerian (ALE) formulation for bodies in rolling contact, as proposed by Nackenhorst (6), is used. Here, the steady-state material flow of the tire material is modeled in a Eulerian (i.e. spatial) formulation (material streamlines). The deformation of the Eulerian domain (i.e. the finite element mesh) is described using a material/Lagrange formulation. As a result, the tire mesh does not rotate and needs only to be refined in the tire/road contact area (6). The rolling contact between the tire and coarse road surface is modeled using a penalty method constraint-based contact mechanics approach (7). The constraint-based computational mechanics method requires no measurements and/or tuning, thus allowing a fully predictive numerical approach. Following the ALE approach, the road surface is modeled as flowing through the spatial tire domain. Given the hub velocity of the rolling tire and a scan of the road surface (or analytical expression of the surface), the road surface asperity heights in spatial points of the tire domain can be extracted per discrete timestep via e.g. a projection based contact detection algorithm (7). This concept is illustrated in Figure 1 (a). These asperity heights are applied in the tire spatial points as geometrical contact constraints $\mathbf{x}_{\mathbf{r}}$ per discrete timestep. Figure 1 (b) shows the time history of the geometrical contact constraints in a tire spatial point, derived from a coarse surface scan.

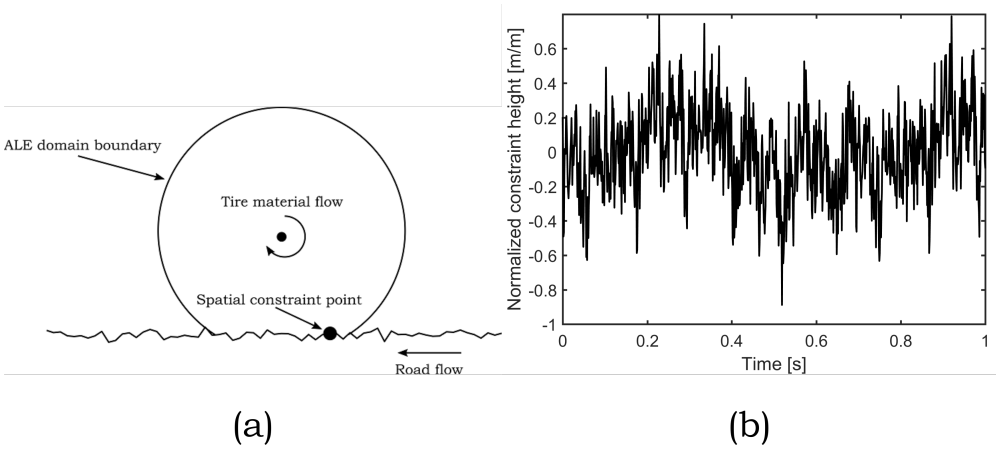

Figure 1. Schematic overview of applying dynamic contact constraints in the ALE-formulation (a) and an example of geometrical contact constraints extracted in a spatial point (b)

In case rim flexibility is considered as well, the structural equations of motion (1) are extended to include the flexible rim domain. Tied contact is assumed between tire and rim in the tire/rim interface, as no relative movement of the tire bead area with respect to the rim flanges typically occurs for steady-state rolling.

In order to include the acoustic wave propagation in the rotating air cavity, the convected Helmholtz equation (8) is used, similar to the work by Cao and Bolton (9):

$$\left(\frac{\partial}{\partial t} + \mathbf{v_0} \cdot \nabla\right)^2 p - c^2 \nabla^2 p = 0 \tag{2}$$

Here, $\mathbf{v_0}$ is the uniform flow velocity (i.e. space- and time independent), ∇ is the Nabla/Del operator [1], c is the speed of sound and p is the acoustic pressure. Information on the weak form of the convected Helmholtz equation and its discretization can be found in e.g. the work by Guasch and Codina (13). While the convected Helmholtz equation assumes uniform flow, the air cavity flow velocity is not constant: it increases linearly across the cavity cross section with respect to the distance from the tire hub. This error is assumed to be of minimal influence for the first acoustic eigenmodes. Similarly to the structural eigenmodes, the acoustic eigenmodes also split-up into traveling modes due to the rotation (1). Applying the vibro-acoustic coupling boundary conditions (14) to the structural equations of motion (1) and including the convected Helmholtz equation then yields the following vibro-acoustic equations of motion:

$$\begin{bmatrix} \mathbf{M} & \mathbf{0} \\ \mathbf{M_{sa}} & \mathbf{M_a} \end{bmatrix} \begin{bmatrix} \ddot{\mathbf{x}} \\ \ddot{\mathbf{p}} \end{bmatrix} + \begin{bmatrix} \mathbf{G_{ALE}} & \mathbf{0} \\ \mathbf{0} & \mathbf{G_a} \end{bmatrix} \begin{bmatrix} \dot{\mathbf{x}} \\ \dot{\mathbf{p}} \end{bmatrix} + \begin{bmatrix} \mathbf{K_{sa}} \\ \mathbf{K_a} - \mathbf{K_{Ga}} \end{bmatrix} \begin{bmatrix} \mathbf{u} \\ \mathbf{p} \end{bmatrix} + \begin{bmatrix} \mathbf{f} - \mathbf{f_{ALE}} \\ \mathbf{0} \end{bmatrix} = \begin{bmatrix} \mathbf{f_p} + \mathbf{f_c} + \mathbf{f_e} \\ \mathbf{0} \end{bmatrix} \tag{3}$$

Here $\mathbf{p} \in \mathbb{R}^{n_a}$ is the air cavity acoustic pressure field, $\dot{\mathbf{p}}$ and $\ddot{\mathbf{p}}$ are its first and second derivatives with respect to time, respectively. Note that all of the dependencies of the structural domain force and matrix terms have been dropped for simplicity of notation. The acoustic mass matrix is denoted as $\mathbf{M_a} \in \mathbb{R}^{n_a \times n_a}$, the acoustic Gyroscopic matrix is denoted as $\mathbf{G_a} \in \mathbb{R}^{n_a \times n_a}$, the acoustic stiffness matrix is denoted as $\mathbf{K_a} \in \mathbb{R}^{n_a \times n_a}$ and the acoustic Gyroscopic stiffness matrix is denoted as $\mathbf{K_{Ga}} \in \mathbb{R}^{n_a \times n_a}$. The vibro-acoustic coupling terms are denoted by $\mathbf{K_{sa}} \in \mathbb{R}^{n \times n_a}$ and $\mathbf{M_{sa}} \in \mathbb{R}^{n_a \times n}$. Additional information on the weak form and discretization of these additional acoustic domain terms and vibro-acoustic coupling terms can be found in the work by Everstine (14). A nonlinear vibro-acoustic FE tire model, as used in this work, is shown in Figure 2.

[1] $\nabla = \left(\frac{\partial}{\partial x_1}, \frac{\partial}{\partial x_2}, \frac{\partial}{\partial x_3}\right)$, where x_i represents a Cartesian coordinate direction

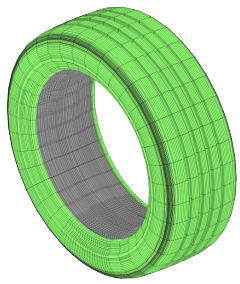

Figure 2. Nonlinear FE tire model as used in this work, where the structural tire domain is shown in green and the acoustic domain is shown in gray

3 APPLICATION OF THE MEM METHOD

In order to reduce the numerical costs associated with solving the nonlinear vibro-acoustic equations of motion (3), which can exceed several weeks of computation time to simulate one second of rolling, the Multi-Configuration Modal (MEM) hyper-reduction method (11) is applied. Using the Galerkin method, a trial solution residing in a lower dimensional subspace of the original solution space is inserted into the equations of motion. Using the same trial solutions, the residual arising due to the insertion of the trial solutions into the equations of motion is eliminated via the projection (i.e. pre-multiplication) of the equations of motion onto the subspace. This yields a lower dimensional system (typically several orders of magnitude smaller), resulting in computational speedups (since a much smaller system needs to be solved). For the nonlinear vibro-acoustic FE tire model, the full-order solution $\begin{bmatrix}\mathbf{u} & \mathbf{p}\end{bmatrix}^T \in \mathbb{R}^{n+n_a}$ is approximated by a reduced-order solution $\begin{bmatrix}\mathbf{q_s} & \mathbf{q_a}\end{bmatrix}^T \in \mathbb{R}^m$, which resides in a constant subspace of the solution space. The subspace is spanned by the columns of $\mathbf{V} \in \mathbb{R}^{n+n_a \times m}$, where:

$$\mathbf{V} = \begin{bmatrix}\mathbf{V_s}^T & \mathbf{V_a}^T\end{bmatrix}^T \tag{4}$$

Here $\mathbf{V_s} \in \mathbb{R}^{n \times m}$ is defined as the structural part of the subspace basis (i.e. approximating the structural field variables) and $\mathbf{V_a} \in \mathbb{R}^{n_a \times m}$ is defined as the acoustic part of the subspace basis (i.e. approximating the acoustic field variables). Hereafter $\mathbf{V}$ is called the reduced order basis (ROB). This leads to the following approximations:

$$\mathbf{x} \approx \tilde{\mathbf{x}} = \mathbf{x_0} + \mathbf{V_s}\mathbf{q_s} \tag{5}$$

$$\mathbf{p} \approx \tilde{\mathbf{p}} = \mathbf{V_a}\mathbf{q_a} \tag{6}$$

Exploiting the ALE-formulation, i.e. the non-rotating mesh, nonlinear static contact configurations and eigenmodes, calculated around these nonlinear static contact configurations, are used as the ROB. The nonlinear static contact configurations capture the gross nonlinear deformation of the tire and are calculated using equidistant samples taken from the a-priori known geometrical road surface constraints. The eigenmodes capture the dynamic response of the tire. Using the finite element assembly procedure, the projected nonlinear terms can be expressed and approximated as (11, 15):

$$\tilde{\mathbf{f}}(\mathbf{x}) = \mathbf{V_s}^T\mathbf{f}(\mathbf{x}) = \sum_{i=1}^{|E|} \mathbf{V_s}_{,i}^T\mathbf{f}_i(\mathbf{x}) \approx \bar{\mathbf{f}}(\mathbf{x}) = \sum_{i=1}^{|E^s|} s_i\mathbf{V_s}_{,i}^T\mathbf{f}_i(\mathbf{x}) \quad \text{and} \quad s_i \geq 0 \tag{7}$$

Here E is the total set of finite elements and $\mathbf{V_s}_{,i}^T$ and $\mathbf{f}_i$ both have a sparse structure, only containing the contributions of element i. A subset of elements $E^s \subset E$ is sampled from the finite element mesh, where $|E^s| \ll |E|$. Each element of the subset E_s is given a positive weight s. Only a limited set of elements thus needs to be evaluated per iteration step to approximate the projected terms. This effectively results in a substantial reduction of the overall computational time. The nonlinear static contact configurations, as used for the ROB, are used

for the element sampling as well. More specifically, a constrained L_1 optimization problem is solved (11). As both the ROB and the MEM method only require static configurations (and eigenmodes calculated around these configurations), the overall MOR approach is feasible to use in a design context, as all static configurations can be calculated in parallel and no dynamic simulations of the full-order model are required. Application of the MEM hyper-reduction method to expression (3) then yields:

$$\tilde{\mathbf{M}} \begin{bmatrix} \ddot{\mathbf{q}}_\mathbf{s} \\ \ddot{\mathbf{q}}_\mathbf{a} \end{bmatrix} + \bar{\mathbf{G}} \begin{bmatrix} \dot{\mathbf{q}}_\mathbf{s} \\ \dot{\mathbf{q}}_\mathbf{a} \end{bmatrix} + \tilde{\mathbf{K}}_\mathbf{sa} \begin{bmatrix} \mathbf{q}_\mathbf{s} \\ \mathbf{q}_\mathbf{a} \end{bmatrix} = \bar{\mathbf{f}} \tag{8}$$

Here the reduced and hyper-reduced terms are:

$$\tilde{\mathbf{M}} = \begin{bmatrix} \mathbf{V_s}^T \mathbf{M} \mathbf{V_s} & \mathbf{0} \\ \mathbf{V_a}^T \mathbf{M_{sa}} \mathbf{V_s} & \mathbf{V_a}^T \mathbf{M_a} \mathbf{V_a} \end{bmatrix} \in \mathbb{R}^{m \times m} \tag{9}$$

$$\tilde{\mathbf{G}} = \begin{bmatrix} \mathbf{V_s}^T \mathbf{G_{ALE}} \mathbf{V_s} & \mathbf{0} \\ \mathbf{0} & \mathbf{V_a}^T \mathbf{G_a} \mathbf{V_a} \end{bmatrix} \in \mathbb{R}^{m \times m} \tag{10}$$

$$\tilde{\mathbf{K}}_\mathbf{sa} = \begin{bmatrix} \mathbf{V_s}^T \mathbf{K_{sa}} \mathbf{V_a} \\ \mathbf{V_a}^T \left(\mathbf{K_a} - \mathbf{K_{Ga}} \right) \mathbf{V_a} \end{bmatrix} \in \mathbb{R}^{m \times m} \tag{11}$$

$$\tilde{\mathbf{f}} = \begin{bmatrix} \mathbf{V_s}^T \left(\mathbf{f_p} + \mathbf{f_c} + \mathbf{f_e} - \mathbf{f} \right) \\ \mathbf{0} \end{bmatrix} \in \mathbb{R}^{m} \tag{12}$$

$$\bar{\mathbf{G}} = \begin{bmatrix} \sum_{i=1}^{|E^s|} s_i \mathbf{V}_{\mathbf{s},i}^T \mathbf{G}_{i,\mathbf{ALE}} \mathbf{V}_{\mathbf{s},i} & \mathbf{0} \\ \mathbf{0} & \mathbf{V_a}^T \mathbf{G_a} \mathbf{V_a} \end{bmatrix} \tag{13}$$

$$\bar{\mathbf{f}} = \begin{bmatrix} \sum_{i=1}^{|E_p^s|} s_{i,\mathbf{p}} \mathbf{V}_{\mathbf{s},i}^T \mathbf{f}_{i,\mathbf{p}} + \mathbf{V_s}^T \mathbf{f_c} + \mathbf{V_s}^T \mathbf{f_e} - \sum_{i=1}^{|E^s|} s_i \mathbf{V}_{\mathbf{s},i}^T \left(\mathbf{f}_i - \mathbf{f}_{i,\mathbf{ALE}} \right) \\ \mathbf{0} \end{bmatrix} \tag{14}$$

4 APPLICATION OF THE PREDICTIVE METHODOLOGY

A tire of size 205/55R16 mounted on a lightweight alloy rim is loaded force-controlled, using a vertical external force $||\mathbf{f_e}||$ = 4000N, onto a drum. After achieving the desired static vertical load, the axle position is locked and the drum is set into motion. The drum rotates with a fixed angular velocity and drives the tire. The drum angular velocity is chosen such that the rolling speed of the tire is 22.22ms^{-1}, i.e. 80kmh^{-1}. A coarse road surface is mounted on the drum. A fully nonlinear vibro-acoustic FE model of the test tire is constructed using geometrical properties extracted from the test tire design and material properties extracted from material tests. This full order model (FOM) contains over 38,000 elements and 175,000 degrees of freedom (DOFs). Using the ROB and the MEM hyper-reduction method, a hyper-reduced order model (HROM) of the FOM is created. The number of degrees of freedom (DOFs) is reduced by a factor of 125, whereas the number of elements that have to be evaluated per iteration step ($|E|$ or $|E_s|$) has been reduced by a factor 27. The total speedup factor (SF) after application of the MEM method is in the order of magnitude of 100. The full-order approach takes around ten to eleven times longer than the experimental approach, while the MOR approach is typically ten times faster than the experimental approach. This effectively means that the total simulation time is reduced from months to hours. A total of one second of rolling is considered in order to achieve a relevant frequency resolution. Since steady-state rolling is considered, spectral convergence is achieved for even this duration of rolling.

As an application case, the influence of the inflation pressure on the vertical hub force spectrum and corresponding structure-borne interior noise is investigated. Two different inflation pressures, $p_a = 2 \cdot 10^5$Pa and $p_a = 2.5 \cdot 10^5$Pa are considered. The shift of certain peaks in the 50–200Hz frequency range is of interest to assess the effect of the inflation pressure. A comparison between the experimental and numerical results is shown in Figure (3). The $p_a = 2 \cdot 10^5$Pa and $p_a = 2.5 \cdot 10^5$Pa cases are shown in Figure (3) (a) and (b), respectively. The vertical hub force spectra are predicted with good accuracy, and therefore allow to use the proposed predic-

tive methodology as an alternative to experimental approaches to assess the structure-borne noise performance of a tire design.

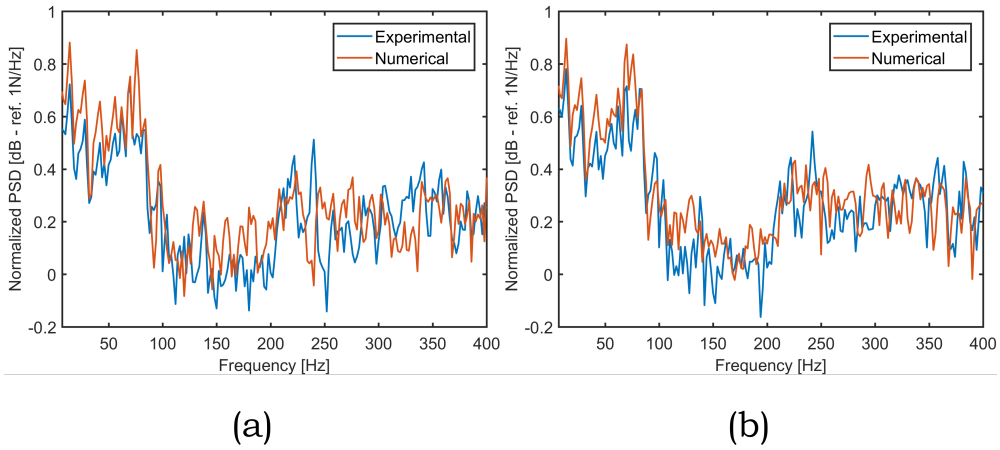

Figure 3. Comparison of the normalized experimental and numerical vertical hub force PSDs, for two different inflation pressures: $p_a = 2 \cdot 10^5$Pa (a) and $p_a = 2.5 \cdot 10^5$Pa (b)

Effects and limitations of modeling assumptions

Including all nonlinearities in the equations of motion (3) results in the need for MOR and hyper-reduction. An alternative could be to linearize the equations of motion (keeping only the contact force term nonlinear) in order to reduce the numerical costs. The vertical hub force Power Spectral Density (PSD) corresponding to this case is shown in Figure 4 (a), along with the vertical hub force PSD for the fully nonlinear case (i.e. keeping all nonlinear dependencies). As can be seen, the nonlinearities need to be taken into account in order to have a fully predictive methodology for the entire frequency range of interest, as the linearized approach is limited to lower frequencies and therefore less suitable for a structure-borne interior noise prediction application.

For 15 – 17 inch passenger car tire sizes, alloy rims typically have a limited influence on the vertical hub force spectrum, as the (radial) rim dynamics are out of the 0–400Hz frequency range (16). While of less interest for structure-borne interior noise prediction, the lateral hub force spectrum typically is influenced by the rim dynamics in the frequency range of interest, even for alloy rims in the 15–17 inch size range. The effect of including a 16 inch flexible alloy rim model on the lateral hub force spectrum is shown in Figure (4) (b). As can be seen, the coupling between the flexible alloy rim and the tire and its effect on the lateral hub force is not negligible. When considering either steel rims of comparable size or larger size alloy rims, both of which have their resonance frequencies typically below 350Hz, the vertical hub force spectrum is therefore influenced by the rim dynamics as well and a flexible rim model should then be included to capture these effects in order to accurately predict the vertical hub forces and corresponding structure-borne interior noise.

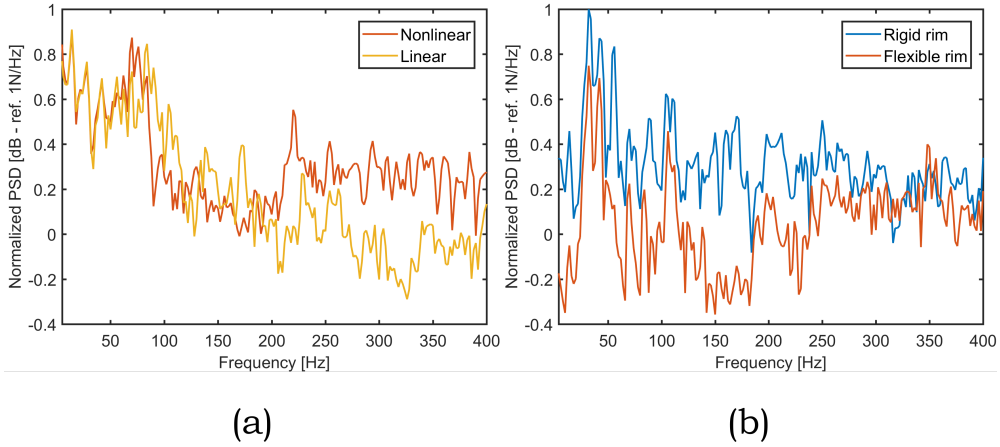

Figure 4. Influence of the nonlinear terms on the simulated vertical hub force PSD (a) and the influence of including a flexible rim model on the simulated lateral hub force PSD (b)

5 CONCLUSIONS

In this work, the use of a high-fidelity approach for predicting the tire/road contact and corresponding hub forces for constant speed rolling over a coarse road surface is described. Vertical hub forces are typically a the main source of structure-borne interior noise when rolling over a coarse road surface, prediction of these hub forces therefore allows to assess the interior noise performance of a tire design. A fully nonlinear FE tire model (which can be seen as a Digital Twin) is combined with an ALE-formulation and a constraint based contact mechanics formulation. The acoustic domain is modeled using the convected Helmholtz equation. In order to reduce the computational costs associated with solving the set of nonlinear equations of motion, the MEM hyper-reduction method is applied. Speedup factors of about 100 are achieved, effectively reducing the computation time from months to hours.

The influence of the inflation pressure on the structure-borne interior noise performance of a tire is investigated as an application case. Both a physical test tire and numerical test tire are loaded onto a rolling drum with a coarse surface. The vertical hub force spectra are calculated and compared for both the physical and numerical test tire for two different inflation pressures. A good correspondence can be observed between the experimental and numerical results. The described predictive methodology can therefore be used as an alternative to the experimental approach, in order to assess the structure-borne interior noise performance. While for the tire considered in this work the dynamic properties of the alloy rim have a limited influence on the vertical hub force spectrum in the 0–400Hz frequency range of interest, it is shown that for the lateral hub force spectrum the influence is not negligible. In general, a flexible rim model should be included for steel rims of comparable sizes, as well as for larger sized alloy rims. Inclusion of the nonlinear terms in the equations of motion is necessary to correctly predict the vertical hub force spectrum in the entire frequency range of interest, as a linearized approach is limited to lower frequencies.

ACKNOWLEDGEMENTS

The research of Daniel De Gregoriis is funded by an AFR-PhD grant supported by the Fonds National de la Recherche, Luxembourg (AFR PhD Grant Agreement PhD 2015-1, Project Reference 10222097). The Fund for Scientific Research - Flanders (F.W.O.) is gratefully acknowledged for the support of the postdoctoral research of Frank Naets. The Industrial Research Fund KU Leuven is gratefully acknowledged for its support.

REFERENCES

[1] Vercammen, S. Tyre/road noise due to road surface texture excitations: Experimental and numerical analyses. KU Leuven, Leuven (Belgium), 2017.

[2] Sakata, T.; Morimura, H.; Ide, H. Effects of Tire Cavity Resonance on Vehicle Road Noise. Tire Science and Technology, Vol 18 (2), 1990, pp 68-79.

[3] Kim, B. S; Kim, G. J.; Lee, T. K. The identification of tyre induced vehicle interior noise. Applied Acoustics, Vol 68 (1), 2007, pp 134-156.

[4] Hartleip, L.; Roggenkamp, T. Case Study - Experimental Determination of Airborne and Structure-borne Road Noise Spectral Content on Passenger Vehicles. SAE Technical Paper 2005-01-2522, 2005.

[5] De Gregoriis D.; Naets F.; Kindt P.; Desmet W. Development and validation of a fully predictive high-fidelity simulation approach for predicting coarse road dynamic tire/road rolling contact forces. Journal of Sound and Vibration, Vol 452, 2019, pp 147-168.

[6] Nackenhorst, U. The ALE-formulation for bodies rolling contact: Theoretical foundations and finite element approach. Computer Methods in Applied Mechanics and Engineering, Vol 198 (39), 2004, pp 4299-4322.

[7] Wriggers, P. Computational Contact Mechanics. Springer-Verlag, Berlin (Germany), 2nd edition, 2006.

[8] Rienstra, S. W.; Hirschberg, A. An Introduction to Acoustics. Technische Universiteit Eindhoven, Eindhoven (The Netherlands), 2004.

[9] Cao, R.; Bolton, J. S. Improved model for coupled structural-acoustic modes of tires. SAE Int. J. Passeng. Cars - Mech. Syst., Vol 8 (3), 2015, pp 845-854.

[10] Van der Auweraer, H.; Donders, S.; Hartmann, D.; Desmet, W. Simulation and digital twin for mechatronic product design. Proceedings of ISMA2018 and USD2018, Leuven (Belgium), 17-19 September 2018, pp 3547-3566.

[11] Naets, F.; De Gregoriis, D.; Desmet, W. Multi-expansion modal reduction: A pragmatic semi-a priori model order reduction approach for nonlinear structural dynamics. International Journal for Numerical Methods in Engineering, in press.

[12] Zienkiewicz, O. C.; Taylor, R. L.; Fox, D. D. The Finite Element Method for Solid and Structural Mechanics, Butterworth-Heineman, Oxford (UK), 7th Edition, 2013.

[13] Guasch, O.; Codina, R. An algebraic subgrid scale finite element method for the convected Helmholtz equation in two dimensions with applications in aeroacoustics. Computer Methods in Applied Mechanics and Engineering, Vol 196 (45), 2007, pp 4672 - 4689.

[14] Everstine, G. Finite element formulatons of structural acoustics problems. Computers & Structures, Vol 65 (3), 1997, pp 307-321.

[15] Farhat, C.; Avery, P.; Chapman, T.; Cortial, J. Dimensional reduction of nonlinear finite element dynamic models with finite rotations and energy-based mesh sampling and weighting for computational efficiency. International Journal for Numerical Methods in Engineering, Vol 98 (9), 2014, pp 625-662.

[16] Wheeler, R. L.; Dorfi, H. R.; Keum B. B. Vibration modes of radial tires: Measurement, prediction, and categorization under different boundary and operating conditions. SAE Technical Paper 2005-01-2523, 2005.